CHAPTER II

THEORITICAL BACKGROUND

In an optical coherence tomography (OCT) system, a coherence length of light source is an important parameter to describe a great significant result. Thus, a low coherence light, which its coherence length is a few micrometer lengths, is used as a light source in the OCT system to investigate a surface profile of an object in a micro- or even nanometer scale. In this chapter, characteristics of low coherence light, used in this research, were first described. Next, an interference of this light by using the Michelson interferometer would be discussed. Finally, a principle of a continuous wavelet transform (CWT) for analyzing interferogram, which was detected from the OCT system, and a method to define thickness of one layer transparent material, which its interferogram from its surface was rarely detected, were introduced.

2.1 Low Coherence Light

Coherence is a correlation between phases of monochromatic light. Light with constant phases is called "completely coherence light", whereas light with random phases is called "completely incoherence light". In case of a perfect monochromatic light, its frequency bandwidth ($\Delta\upsilon$) is zero or an inversion of frequency bandwidth is infinite.

Generally, light is not perfect monochromatic because a source emits a sequence of harmonic wavetrains with finite time that discontinue in phase as shown in Figure 2.1 [12].

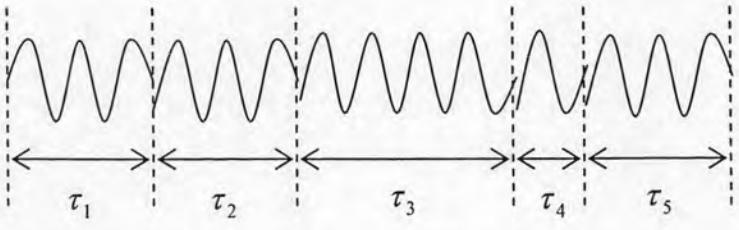

Figure 2.1: The wavetrains with different life time

In case of non-perfect monochromatic light, its frequency bandwidth is not zero, thus, an inversion of frequency bandwidth, known as a coherence time (τ_C), becomes a finite value. Coherence time means an average of the life time. Light, that its frequency bandwidth is not zero or its coherence is partial coherence, is called quasimonochromatic. In the other word, the coherence time is an interval time, which a phase of light can be predicted at any point in space, comparing with the reference point. The quasimonochromatic light also behaves as the monochromatic light, in case the interested interval time is shorter than its coherence time [13]. The coherence length (L_C) can be expressed as:

$$L_C = c\tau_C, \tag{2.1}$$

where c is the velocity of light in free space.

Light, having an extra-short of coherence length in order of a few micrometers, is specially called low coherence light. The temporal characteristic curve between an optical path difference (Δp) of the low coherence light and its coherence length can be defined as in Figure 2.2. According to the characteristic curve in Figure 2.2, the Δp, having the highest intensity, is the position that a sample surface and a reference surface are in the same position when the Michelson interferometer is considered.

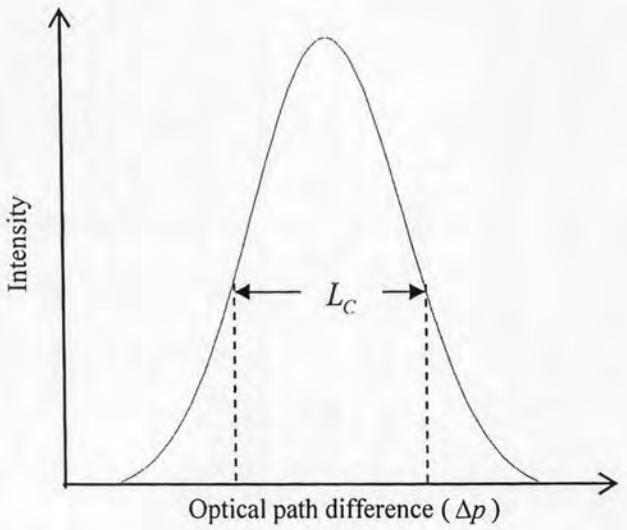

Figure 2.2: Temporal characteristic curve between the optical path difference (Δp) and light intensity.

With low coherence interferometry (LCI) technique, this low coherence light can be applied to extract an adjacent layer in a multi-layer material, since a distance between these two layers is less than the coherence length of this light source. In case the distance between the layer and the next layer is more than L_C, the Δp, having the highest intensity, is very close together. Therefore, two highest intensity positions are hardly defined. That leads to a lack of some layers. Thus, the coherence length is a key to describe a resolution of an image constructed by the LCI technique. The examples of some low coherence light sources are shown in Table 2.1.

Table 2.1: Example of some low coherence light sources [5].

Light source	Center wavelength ($\bar{\lambda}$)	Wavelength bandwidth ($\Delta\lambda$)	Coherence length (L_C)	Power
Superluminescent diode (SLD)	675 nm	10 nm	20 μm	40 mW
	820 nm	20 nm	15 μm	50 mW
	820 nm	50 nm	6 μm	6 mW
	930 nm	70 nm	6 μm	30 mW
	1300 nm	35 nm	21 μm	10 mW
	1550 nm	70 nm	15 μm	5 mW
Light emitting diode (LED)	1240 nm	40 nm	17 μm	0.1 mW
	1300 nm	40 nm	17 μm	0.1 mW
Superfluorescence				
Yb-doped fiber	1064 nm	30 nm	17 μm	40 mW
Er-doped fiber	1550 nm	80-100 nm	16 μm	100 mW
Tm-doped	1800 nm	80 nm	18 μm	7 mW
Photonic crystal fiber	1.3 μm	370 nm	2.5 μm	6 mW
	725 nm	370 nm	0.75 μm	6 mW

The coherence can be defined into two types, temporal coherence and spatial coherence. For temporal coherence, light interferes with a delayed version of itself.

That means amplitude splitting is considered. For spatial coherence, the light interferes with a spatially shifted version of itself. In this case wavefront splitting is considered. These ideas lead to a concept of a mutual coherence function for describing correlations between phases of the light. This function will be explained in section 2.3.

In this research, a superluminescent diode (SLD) is used as the low coherence light source. Although the SLD has a large of coherence length than the others, its system is not complication to use. It is also the light source that has low heat, compact size and economic cost. Moreover, some researchers developed a new technique to combine the multi-SLD for increasing a resolution of result image, having a better image quality and a fine cross-sectional structure imaging [14]. Thus, a basic knowledge of the SLD in OCT is an important thing for developing the OCT method in the future.

2.2 The Michelson Interferometer

The Michelson interferometer was introduced by Albert Michelson in 1881. More than two centuries, this interferometer has been proved that it is important tool for developing the modern physics, such as the standard of meter by using the wavelength of light and the tidal effect of the moon on the earth [12]. A schematic of the Michelson interferometer is shown in Figure 2.3.

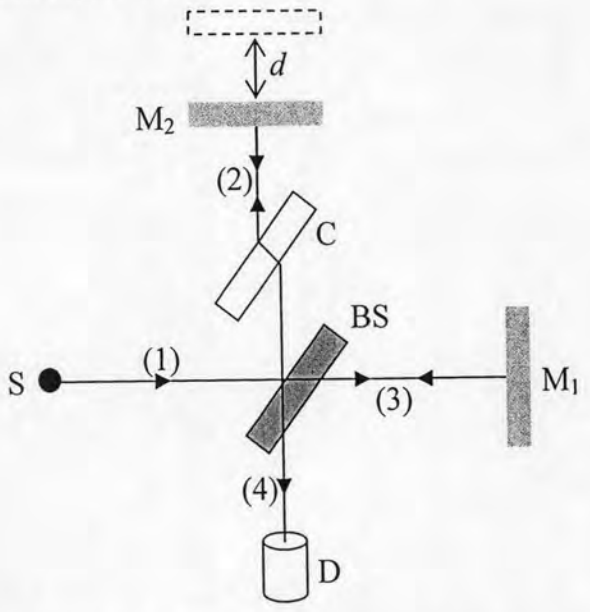

Figure 2.3: The Michelson interferometer

Light from source S travels to a beamsplitter BS, then, an original light is split into two parts, beam (2) and beam (3). These two beams separately travel to each arm of this interferometer. The beam (3) incidents and reflects from a fixed mirror M_1. Then, the reflected light travels to the beamsplitter again and it reflects the light to a detector D. The beam (2) incidents and reflects from a movable mirror M_2 and then it travels to the beamsplitter in the same way. A combination of beam (2) and beam (3) is beam (4). Because of an optical path difference of beam (2) and beam (3), interference patterns will be occurred. A compensator C is used for assuring that the light in both arms travels in glass with the same optical path length. In real system, one mirror, replaced by the sample, is called the sample arm. Another is called the reference arm. The light, reflected from the movable mirror M_2, has only delay of itself, comparing with the reflected light from the fixed mirror M_1. This kind of interferometer is one of the examples of amplitude splitting interferometer.

For convenience, two optical axes of the Michelson interferometer can be considered as equivalent optical system in one axis, shown in Figure 2.4.

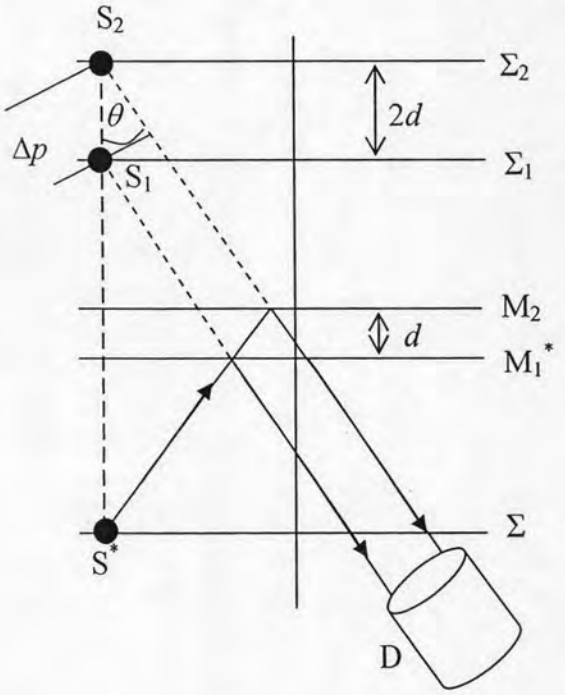

Figure 2.4: Equivalent optical system in one axis of the Michelson interferometer

The fixed mirror M_1 and the source S, as shown in Figure 2.3, are rotated counterclockwise 90°. The source S is replaced by a virtual source S^* from a beamsplitter plane Σ. The M_1^* is a new position of the fixed mirror M_1. A position of the movable mirror M_2 can be in front of, behind or coincident with the fixed mirror M_1^*. The light from the virtual source S^* is reflected from both mirror M_1^* and M_2 with path difference d. The two reflected beams at the detector D come from two virtual images S_1 and S_2 as the image plane Σ_1 and Σ_2, respectively. The distance between two mirrors is a half of the distance between the image planes, because the light incidents and reflects from the mirror. The optical path difference (Δp) of this interferometer is

$$\Delta p = 2d\cos\theta \tag{2.2}$$

where θ is an angle of the beams that relate to the axis.

The interference patterns can be observed when the optical path difference is smaller than the coherence length of light. For low coherence light, interference patterns can be observed in a few micrometer scales. In case a started position of the movable mirror M_2 is set in front of the fixed mirror M_1^* and then it is moved behind the mirror M_1^*, interference patterns on the detector will pass from a constructive state to a destructive state and so on. The intensity, detected by the detector, varies with the position of the movable mirror M_2, as in Figure 2.5.

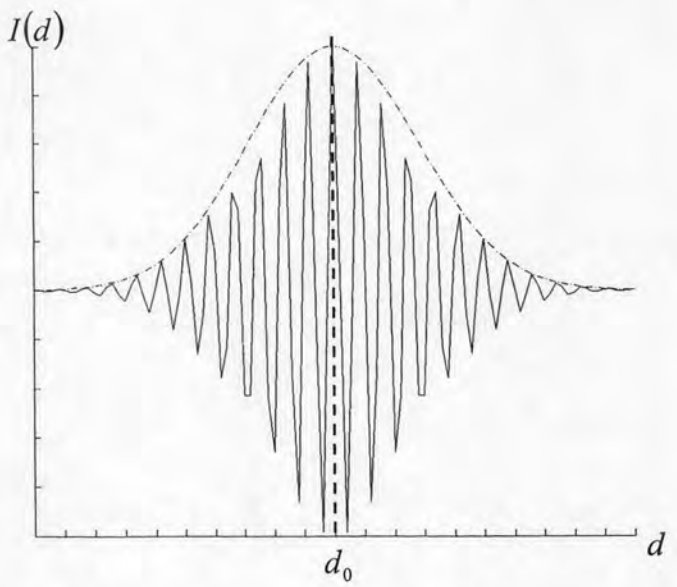

Figure 2.5: Intensity signals at any movable mirror position

The interference patterns of the intensity signals, varying with the position as shown in Figure 2.5, are called "interferogram". The position d_0 is the position that is no path differences between two mirrors. Therefore, the maximum intensity of the interference patterns occurs; in the other word, a large interference signal can be produced. The intensity gradually decreases from the position d_0 because of a decreasing of phase correlations between two beams. When path difference of two beams is larger than the coherence length of light, there is no more correlation between time delays or phases of two beams. The interference patterns cannot be observed and the intensity of the interferogram is an average value.

2.3 Mathematical Description of the Interfeogram

In Figure 2.6, a point source S is a monochromatic light source. It generates light propagating to an aperture S_1 and S_2. Since the aperture S_1 and S_2 are isolated, S_1 and S_2 are two new light sources. Thus, they cause an interference at point P because of the path difference between S_1 and S_2.

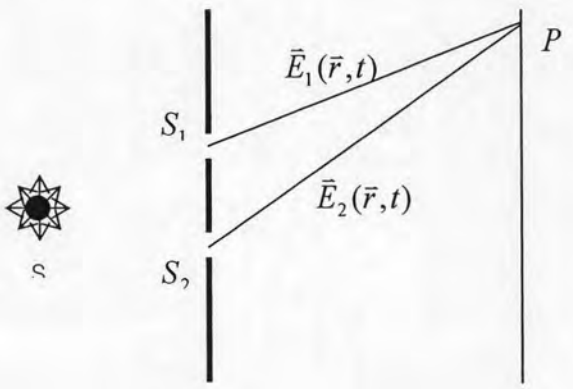

Figure 2.6: Interference at point P by aperture S_1 and S_2

An electric field of these two new light sources, S_1 and S_2, are given by [12]:

$$\vec{E}_1(\vec{r},t) = \vec{E}_{01}\exp[i(\vec{k}_1 \bullet \vec{r} - \omega t + \varepsilon)], \tag{2.3}$$

$$\vec{E}_2(\vec{r},t) = \vec{E}_{02}\exp[i(\vec{k}_2 \bullet \vec{r} - \omega t + \varepsilon)], \tag{2.4}$$

where $\vec{E}_{01}$ and $\vec{E}_{02}$ are an amplitude of $\vec{E}_1(\vec{r},t)$ and $\vec{E}_2(\vec{r},t)$, respectively,

$\vec{k}_1$ and $\vec{k}_2$ are a propagating vector of $\vec{E}_1(\vec{r},t)$ and $\vec{E}_2(\vec{r},t)$, respectively,

$\vec{r}$ is a position vector,

ω is an angular frequency,

t is a time and

φ is an initial phase.

At point P, the electric filed is only varied on time. A lower path ($\overline{S_2P}$) is also longer than an upper path ($\overline{S_1P}$) by a time interval (τ). In case the initial phases of these two fields are the same. Thus, Eq.(2.3) and Eq.(2.4) are rewritten as:

$$\vec{E}_1(t) = \vec{E}_{01}\exp[-i\omega t],$$

$$\vec{E}_2(t+\tau) = \vec{E}_{02}\exp[-i\omega(t+\tau)].$$

Also, the electric field at point P is written as:

$$\vec{E}_P(\tau) = \vec{E}_1(t) + \vec{E}_2(t+\tau), \tag{2.5}$$

and a resultant irradiance at point P is

$$I_P = <\vec{E}_P(\tau)\bullet\vec{E}_P{}^*(\tau)>, \tag{2.6}$$

where $<.>$ means a time average and * means a complex conjugate.

Then, Eq.(2.6) can be expressed by:

$$I_P = <\left|\vec{E}_1(t)\right| + \left|\vec{E}_2(t+\tau)\right| + [\vec{E}_1(t)\bullet\vec{E}_2{}^*(t+\tau) + \vec{E}_2(t+\tau)\bullet\vec{E}_1{}^*(t)]>. \tag{2.7}$$

The last term in Eq.(2.7) is a product of a quantity adding its own complex conjugate. This value of this last term is just twice its real part, thus, Eq.(2.7) can be rewritten as:

$$I_P = I_1 + I_2 + 2\,\mathrm{Re} < \vec{E}_1(t)\bullet\vec{E}_2{}^*(t+\tau) >, \tag{2.8}$$

where I_1 and I_2 are the irradiance of $\vec{E}_1(t)$ and $\vec{E}_2(t+\tau)$, respectively.

The third term of Eq.(2.8) is an autocorrelation or cross-correlation function, denoted by:

$$\vec{\Gamma}_{12}(\tau) \equiv < \vec{E}_1(t)\bullet\vec{E}_2{}^*(t+\tau) >, \tag{2.9}$$

and it is known as the mutual coherence function. This function can explain correlations between the electric field from S_1 and S_2 at point P.

If S_1 and S_2 are identical, the mutual coherence function can be written as:

$$\bar{\Gamma}_{11}(\tau) = < \bar{E}_1(t) \bullet \bar{E}_1{}^*(t+\tau) >,$$

or

$$\bar{\Gamma}_{22}(\tau) = < \bar{E}_2(t) \bullet \bar{E}_2{}^*(t+\tau) >.$$

In case, there is no path difference between two fields (τ =0), these functions become

$$\Gamma_{11}(0) = < \bar{E}_1(t) \bullet \bar{E}_1{}^*(t) >= I_1,$$

and

$$\Gamma_{22}(0) = < \bar{E}_2(t) \bullet \bar{E}_2{}^*(t) >= I_2.$$

Hence, these functions are called the self-coherence function.

A normalized form of the mutual coherence function is [6]

$$\bar{\gamma}_{12}(\tau) \equiv \frac{\bar{\Gamma}_{12}(\tau)}{\sqrt{\Gamma_{11}(0)\Gamma_{22}(0)}} = \frac{< \bar{E}_1(t) \bullet \bar{E}_2{}^*(t+\tau) >}{\sqrt{< \left|\bar{E}_1\right|^2 >< \left|\bar{E}_2\right|^2 >}}. \qquad (2.10)$$

This normalized form is known as a complex degree of coherence and then Eq.(2.8) can be rewritten as:

$$I_P = I_1 + I_2 + 2\sqrt{I_1 I_2}\,\mathrm{Re}[\bar{\gamma}_{12}(\tau)], \qquad (2.11)$$

where $\sqrt{< \left|\bar{E}_1\right| >< \left|\bar{E}_2\right| >} = \sqrt{I_1 I_2}$. And Eq.(2.11) is the general interference law of partial coherence.

For quasimonochromatic, a relation of path difference and phase difference are given by:

$$\frac{\varphi}{2\pi} = \frac{(r_2 - r_1)}{\bar{\lambda}},$$

or

$$\varphi = 2\pi\bar{\upsilon}\tau$$

where φ is a phase difference,

$\bar{\lambda}$ is the central wavelength of light,

$\bar{\upsilon}$ is the central frequency of light and

$(r_2 - r_1)$ is the path difference of a lower and upper path that equal to $c\tau$.

The complex degree of coherence is expressed as:

$$\bar{\gamma}_{12}(\tau) = |\bar{\gamma}_{12}(\tau)| \exp\{i[\alpha_{12}(\tau) - \varphi]\} \tag{2.12}$$

where a phase angle of $\bar{\gamma}_{12}(\tau)$ relates to Eq.(2.9) and the phase difference φ of quasimonochromatic. By using this equation, the irradiance at point P from Eq.(2.11) is rewritten as:

$$I_P = I_1 + I_2 + 2\sqrt{I_1 I_2}\,|\bar{\gamma}_{12}(\tau)| \cos[\alpha_{12}(\tau) + \varphi]. \tag{2.13}$$

The term $|\bar{\gamma}_{12}(\tau)|$ is the degree of coherence that can be considered in three cases:

1. In case $|\bar{\gamma}_{12}(\tau)|$=1, the interference is generated from two coherent beams. The cosine term only depends on $\alpha_{12}(\tau)$.
2. In case $|\bar{\gamma}_{12}(\tau)|$=0, that means these two beams are incoherence. Therefore, there are no interference or $I_P = I_1 + I_2$.
3. In case $0<|\bar{\gamma}_{12}(\tau)|<1$, that means the interference is produced from two partial coherence beams. Like the coherent beam, the maximum and minimum of I_P depend on the cosine term.

For the partial coherence, a maximum irradiance is written as:

$$I_P(\max) = I_1 + I_2 + 2\sqrt{I_1 I_2}\,|\bar{\gamma}_{12}(\tau)|,$$

and a minimum irradiance is

$$I_P(\min) = I_1 + I_2 - 2\sqrt{I_1 I_2}\,|\bar{\gamma}_{12}(\tau)|.$$

Then a visibility (V) of interference patterns at point P is

$$V_P = \frac{I_P(\max) - I_P(\min)}{I_P(\max) + I_P(\min)} = \frac{2\sqrt{I_1 I_2}}{I_1 + I_2}|\bar{\gamma}_{12}(\tau)|. \tag{2.14}$$

If $I_1 = I_2$, Eq.(2.14) will be written as:

$$V_P = |\bar{\gamma}_{12}(\tau)|. \tag{2.15}$$

The degree of coherence is the visibility of the interference patterns when the intensity of the original two beams is equal.

For the Michelson interferometer, the two sources S_1 and S_2 as in Figure 2.6 is represented the beams that reflects from the mirror M_1 and M_2, respectively. The point P in the same Figure is replaced with the detector D. Thus, S_1 and S_2 are

identical and the mutual coherence function, $\bar{\Gamma}_{11}(\tau)$ or $\bar{\Gamma}_{22}(\tau)$, will be considered. The normalized of this mutual coherence function becomes [13]:

$$\bar{\gamma}_{11}(\tau) = \frac{\bar{\Gamma}_{11}(\tau)}{\sqrt{<\left|\bar{E}\right|^2><\left|\bar{E}\right|^2>}} = \frac{<\bar{E}(t)\bullet\bar{E}^*(t+\tau)>}{E^2}. \tag{2.16}$$

Eq.(2.16) is called the complex degree of temporal coherence.

In case the electric field of each beam is given by [12]:

$$\bar{E}(t) = E_0 \exp\{-i[\omega t - \varphi(t)]\},$$

where $\varphi(t)$ is a phase of the harmonic wave. Then, Eq.(2.16) can be written as:

$$\bar{\gamma}_{11}(\tau) =< \exp\{i[\varphi(t) - \varphi(t+\tau)]\} > \exp(i2\pi\bar{\upsilon}\tau). \tag{2.17}$$

The time average term of Eq.(2.17) is the magnitude of complex degree of temporal coherence $\left|\bar{\gamma}_{11}(\tau)\right|$, which can be expressed as [5]:

$$< \exp\{i[\varphi(t) - \varphi(t+\tau)]\} >= \frac{1}{T}\int_0^T \exp\{i[\varphi(t) - \varphi(t+\tau)]\}dt.$$

Then Eq.(2.17) can be rewritten as:

$$\bar{\gamma}_{11}(\tau) = \left|\bar{\gamma}_{11}(\tau)\right| \exp(i2\pi\bar{\upsilon}\tau). \tag{2.18}$$

A relation of the complex degree of temporal coherence and the normalized spectral density is given by [15]:

$$\bar{\gamma}_{11}(\tau) = \int_0^\infty \hat{S}(\upsilon)\exp[-i(2\pi\upsilon\tau)]d\upsilon, \tag{2.19}$$

where $\hat{S}(\upsilon)$ is the normalized spectral density.

The spectral density of the superluminescent diode (SLD), used as the light source in this research, is a Gaussian shape that can be expressed by [16]:

$$\hat{S}(\upsilon) \cong \frac{2\sqrt{\ln 2}}{\sqrt{\pi}\Delta\upsilon}\exp\left[-\left(2\sqrt{\ln 2}\bullet\frac{\upsilon-\bar{\upsilon}}{\Delta\upsilon}\right)^2\right], \tag{2.20}$$

where $\Delta\upsilon$ is the frequency bandwidth of light.

After replacing $\hat{S}(\upsilon)$ from Eq.(2.20) in Eq.(2.19) the complex degree of temporal coherence of a Gaussian shape can be calculated from [16]:

$$\bar{\gamma}_{11}(\tau) = \exp\left[-\left(\frac{\pi\Delta\upsilon\tau}{2\sqrt{\ln 2}}\right)^2\right]\exp(i2\pi\bar{\upsilon}\tau). \tag{2.21}$$

If $I_1 = I_2$, the irradiance at the detector D will be written as:

$$I_D(\tau) = I_0 + I_0 V \exp\left[-\left(\frac{\pi\Delta\upsilon\tau}{2\sqrt{\ln 2}}\right)^2\right]\cos(2\pi\bar{\upsilon}\tau), \tag{2.22}$$

where $2I_1 = 2I_2 = I_0$ and V is the visibility.

For the Michelson interferometer, the interval time τ can be expressed by:

$$\tau = \frac{2d}{c},$$

where c is the velocity of light in free space and d is a distance between two arms. Consider z-direction, the distance d is defined as:

$$d = z - z_0,$$

where z_0 is a position that is no path difference between two arms of the Michelson interferometer. Thus, the irradiance at detector can be calculated from a position in z-direction by following the equation [15]:

$$I_D(z) = I_0 + I_0 V \exp\left[-\left(\frac{z - z_0}{L_C}\right)^2\right]\cos\left[\frac{4\pi(z - z_0)}{\bar{\lambda}}\right], \tag{2.23}$$

where L_C is the coherence length of light and $\bar{\lambda}$ is the central wavelength of light. The coherence length can be rewritten as [5]:

$$L_C = \frac{2\ln 2}{\pi}\frac{\bar{\lambda}^2}{\Delta\lambda}, \tag{2.24}$$

where $\Delta\lambda$ is the wavelength bandwidth of light.

2.4 Discrete Fourier Transform and Continuous Wavelet Transform

A continuous Fourier transform is a well known technique to analyze signals. This technique transforms the signals in time domain to frequency domain by breaking down the signals into sinusoid components of different frequencies. In computer calculation, the input and output signals are discrete, thus, the transform is specially used a discrete Fourier transform (DFT). DFT estimates the Fourier transform by using a finite number

of the signals. The symmetry properties of DFT are also like the one of the continuous Fourier transform [17].

By given $x(n)$ as time domain signals and $n = 0...(N-1)$ as an index in time domain, DFT of the signals can be calculated from:

$$\hat{x}(k) = \sum_{n=1}^{N} x(n) \exp\left(-i \frac{2\pi(k-1)(n-1)}{N} \right), \tag{2.25}$$

and the inverse DFT is given by

$$x(n) = \frac{1}{N} \sum_{k=1}^{N} \hat{x}(k) \exp\left(i \frac{2\pi(k-1)(n-1)}{N} \right), \tag{2.26}$$

where k is an index in frequency domain when $k = 0...(N-1)$ and N is the number of signal.

A disadvantage of the Fourier transform is loss of time information. The time information will not be an importance if the signals slowly change in time. But for time varying signals, the information of time is become an important factor. Thus, the Fourier transform is not an efficiency to analyze these signals. To fix this problem, Grossmann and Morlet introduce a new analysis, known as the wavelet transform, which transforms the signals to frequency (scale) domain and time domain by using a wavelet function, called the mother wavelet [18]. There are two types of the wavelet function, orthogonal and nonorthogonal. The former is used with a discrete wavelet transform (DWT), the latter is used both a discrete wavelet transform and a continuous wavelet transform (CWT). This research scopes only the continuous wavelet transform in order to analyze the interferogram that consists of the discrete signals. The result, getting from CWT, will lead to find an actual position, having the maximum intensity.

Because the interferogram has a Gaussian shape, the Morlet wavelet, having a plane wave modulated by a Gaussian, is chosen as the mother wavelet in this research. The Morlet wavelet is expressed by [19]:

$$h(\eta) = \left[\exp(i\omega_0 \eta) - \exp\left(-\frac{\omega_0^2}{2} \right) \right] \exp\left(-\frac{\eta^2}{2} \right), \tag{2.27}$$

where η is a nondimensional time parameter and ω_0 is the nondimensional frequency.

The Fourier transform of Eq.(2.27) can be written as:

$$\hat{h}(\omega) = \sqrt{2\pi}\left\{\exp\left[-\frac{(\omega-\omega_0)^2}{2}\right] - \exp\left(-\frac{\omega_0^2}{2}\right)\bullet\exp\left(-\frac{\omega^2}{2}\right)\right\},$$

and $\hat{h}(\omega) = 0$, since $\omega = 0$. That is $\int_R h(\eta)d\eta = 0$ and Eq.(2.27) is a admissible wavelet that its average is zero [18].

If $\omega_0 = 6$, the term $\exp\left(-\frac{\omega_0^2}{2}\right)$ will become zero and Eq.(2.27) can be written as:

$$h(\eta) = \exp(i\omega_0\eta)\exp\left(-\frac{\eta^2}{2}\right); \quad \omega_0 = 6, \tag{2.28}$$

and this is also admissible wavelet.

The continuous wavelet transform of the signals $y(\eta)$ with the wavelet function $h(\eta)$ is expressed by [20]:

$$W_{a,b}(\eta) = \frac{1}{\sqrt{|a|}}\int_{-\infty}^{\infty} y(\eta)h^*\left(\frac{\eta-b}{a}\right)d\eta.$$

For the interferogram with the discrete signals in z direction, the wavelet transform becomes [21]

$$W_{a,b}(z) = \sqrt{\frac{\Delta z}{|a|}}\sum_{z=0}^{N-1} I_D(z)h^*\left[\left(\frac{z-b}{a}\right)\Delta z\right], \tag{2.29}$$

where a is a scale parameter (compression or expansion the mother wavelet),

b is a translation parameter,

Δz is an increasing step and

N is a number of signals.

Due to the discrete signals of the interferogram, an actual peak may place between an experimental peak and an adjacent point, as shown in Figure 2.7. For CWT, a phase of each peak can be used to calculate the distances between the experimental peak and the actual peak. Because the wavelet transform $W_{a,b}(z)$ consists of real part and imaginary part, the phase φ of the wavelet transform $W_{a,b}(z)$ can be calculated by:

$$\varphi = \tan^{-1}\left(\frac{\mathrm{Im}\{W_{a,b}(z)\}}{\mathrm{Re}\{W_{a,b}(z)\}}\right),$$

and the amplitude of the transform is $\left|W_{a,b}(z)\right|$.

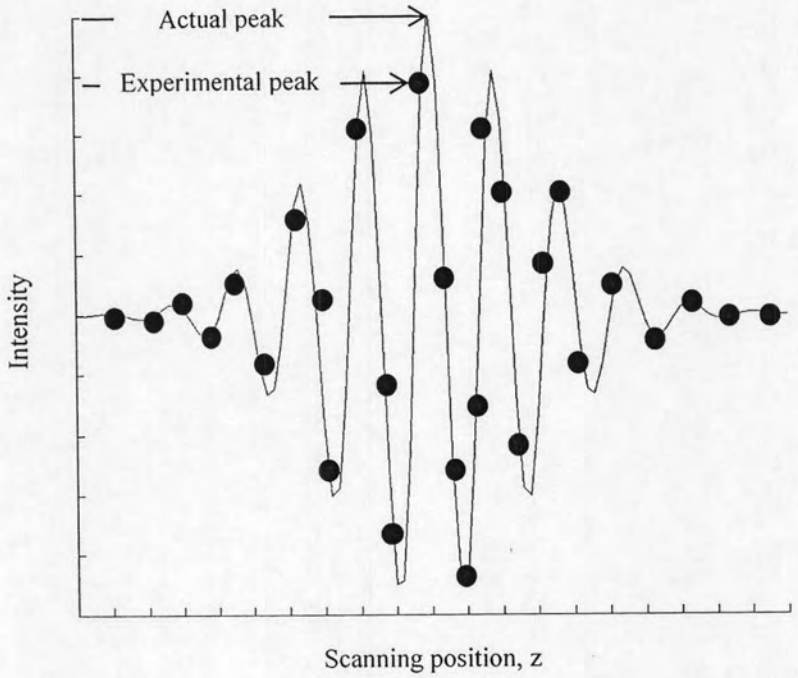

Figure 2.7: Actual peak and experiment peak of interferogram

Thus, a relation of the actual peak and the experimental peak can be written as [11]:

$$\Delta z = z_M - z_R = \frac{\bar{\lambda}}{4\pi}(\varphi - \varphi_0), \tag{2.30}$$

where z_M is a maximum position,

z_R is a real maximum position,

$\bar{\lambda}$ is the central wavelength of light,

φ is a phase of the maximum position from a wavelet analysis and

φ_0 is a phase offset.

A phase of the maximum point (φ) can be found from:

$$\varphi = \tan^{-1}\left(\frac{\mathrm{Im}\{W_{a\_\max,b\_\max}(z)\}}{\mathrm{Re}\{W_{a\_\max,b\_\max}(z)\}}\right),$$

where $a\_\max$ and $b\_\max$ are a position that the amplitude $|W_{a,b}(z)|$ has a maximum value. Because the phase offset is equal to each point of a surface, which can be set in the experimental equipment, thus, the phase offset can be set to become zero and Eq.(2.30) becomes:

$$z_R = z_M - \frac{\overline{\lambda}}{4\pi}\varphi . \tag{2.31}$$

2.5 Method for Defining the Thickness of Transparent Material

In case a surface is covered with a transparent material, intensity of backscattered light from the transparent surface is not strong enough to be detected by CCD camera. Thus, only one interferogram, causing from an inner surface, can be observed. When light passes through a transparent material, its velocity is decrease because of the refractive index of transparent material. That affects to calculated depth of a layer. As the refractive index of transparent material is more than the one of the air, interference patterns from the transparent material surface occur deeper than the ones of the inner surface, as shown in Figure 2.8.

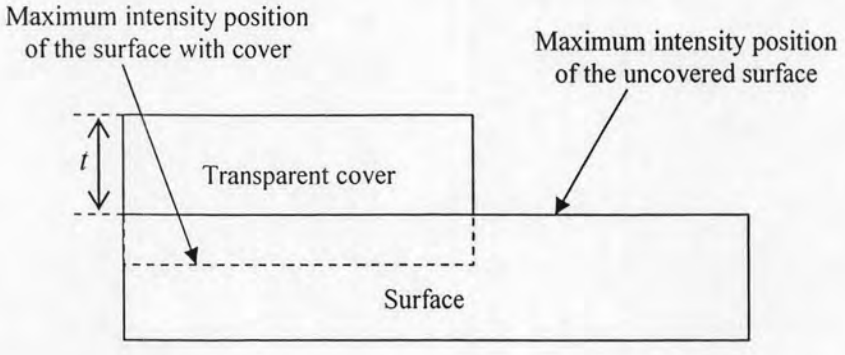

Figure 2.8: A transparent cover on a surface

A thickness t of transparent material can be expressed by [10]:

$$t = \frac{|z_{R1} - z_{R2}|}{n-1}, \tag{2.32}$$

where z_{R1} is a real maximum position of a surface,

z_{R2} is a real maximum position of a surface with a transparent cover and

n is the refractive index of transparent material.